Hindawi
Advances in Materials Science and Engineering
Volume 2022, Article ID 5621154, 11 pages
https://doi.org/10.1155/2022/5621154

Research Article

Adhesion Enhancement on a Duplex DLC HiPIMS Positive Pulse Coating Performed by Active Screen Plasma Nitriding Pretreatment on 316L Stainless Steel Substrate

Iñigo Gómez,[1] **Jose Antonio García**,[1] **Jose Antonio Santiago**,[2] **Iván Fernandez**,[2] **Palacio Jose Fernandez**,[3] **and Iñigo Braceras**[4]

[1]*Engineering Department, Public University of Navarre (UPNA), Campus Arrosadía, 31006 Pamplona, Spain*
[2]*Nano4Energy SL, José Gutiérrez Abascal 2, 28006 Madrid, Spain*
[3]*Centre of Advanced Surface Engineering, AIN, 31191 Cordovilla, Spain*
[4]*Tecnalia, Basque Research and Technology Alliance (BRTA), Mikeletegi Pasealekua 2, Donostia-San Sebastian, Spain*

Correspondence should be addressed to Iñigo Gómez; inigo.gomez@unavarra.es

Received 25 September 2022; Revised 7 November 2022; Accepted 15 November 2022; Published 23 November 2022

Academic Editor: Senthil Kumaran Selvaraj

Diamond-like carbon (DLC) coatings have been the object of research interest due to properties such as excellent wear resistance, low coefficient of friction, high hardness, high elastic modulus, and biocompatibility. Despite this, DLC has poor adhesion properties, which makes it challenging to use in industrial applications. The application of DLC using the high-power pulse magnetron sputtering (HiPIMS) technique with positive pulses has been studied. Seeking greater DLC coating adherence, the application of a nitriding pretreatment prior to the DLC coating has been studied to improve its adhesion to AISI316L stainless steel soft metal substrates, employing active screen plasma nitriding (ASPN). The influence of the different pretreatment temperatures to reach the maximum levels of adhesion has been analyzed. Scratch methods have been employed to assess adhesion. The elemental composition, morphology, and roughness of the samples have been studied, as well as the behavior of resistance to wear and friction. The results show an improvement in DCL adhesion. Critical loads (LC3) increase at higher pretreatment temperatures, from 48 N for the DLC to 82 N for the ASPN + DLC. Pretreatment has also been shown to be effective in maintaining excellent dry wear resistance properties and a low coefficient of friction.

1. Introduction

Human prostheses have a history that exceeds 3,000 years. From the first orthopedic leg prostheses, the functional replicas of amputated fingers, going through the glass cups for the first mold arthroplasties to the hip prostheses manufactured in 3D with a determined porosity to achieve the acceptance of the same by part of the human body [1–5]. Still, they present several shortcomings such as the practical operative life of the implanted devices. Therefore, finding a way for such prosthetic systems to last for a long time is one of the key factors why DLC coatings attract great interest in biomedical applications [6–10].

Its excellent properties such as resistance to wear, low coefficient of friction, and biocompatibility make DLC interesting for its use in elements that will be inserted into the human body, with a low risk of eliciting a foreign body reaction. Likewise, in the case of long-term or permanent implants, a low wear rate and biocompatible, nontoxic, and wear debris are key issues that make DLC potentially a good coating candidate, competing with other surface treatments [11, 12].

However, DLC coatings have a low adhesion strength to metallic substrates, associated with the low density of covalent chemical bonds, which, together with the high compressive stress, makes their use difficult in critical high-tech applications.

Therefore, there is a wide field of study to improve the aforementioned adherence to the metallic substrate [2]. The use of new DLC coating techniques such as the positive pulse HiPIMS opens the door to improving the adhesion of this kind of coating with the use of pretreatments such as active screen plasma nitriding, producing a duplex coating with improved properties [13, 14].

The bonding force difference between the ASPN-substrate and DLC-substrate has been studied. The application of ASPN allows the elimination of drawbacks such as the appearance of the edge effect or the hollow cathode effect that can be caused by conventional plasma nitriding. The ASPN provides an improvement in its behavior of wear and corrosion resistance. The ASPN nitriding pretreatment electrical potential process influences the chemical characteristics, hardness, and tribological behavior of the deposition layers [15–18].

Optimized DLC coating, HiPIMS technology of positive pulses implemented by Santiago et al., has been maintained as a constant in the study. Meanwhile, three temperature conditions of the nitriding pretreatment have been explored to achieve greater adhesion of the resulting duplex coating [19–23].

As seen in previous studies, initial nitriding can lead to an improvement in the adhesion properties of the subsequently deposited film. Although, in the case of austenitic stainless steel, a solution to avoid the chromium nitrides precipitation that would weaken and compromise the corrosion resistance of the alloy must be found at low temperatures [24].

This article focuses on the improvement of DLC coating hardness and wear resistance, increasing the DLC-substrate adherence using ASPN pretreatment at three study temperatures without compromising the corrosion resistance of the stainless steel with chromium precipitation.

2. Results

2.1. Thickness and Composition. The thickness of the DLC films was ≈ 1 μm (Figure 1) in all the samples studied. The thicknesses of the DLC WC : C layers were kept constant at approximately the same proportions in all HiPIMS-treated samples as seen in Figure 2 where the DLC glow-discharge optical emission spectroscopy (GDOES) is shown. The total thickness was determined to be around 1 μm, where the deposition of a chromium layer begins after the argon etching reaches levels of 45 atomic percentage (at.%). The percentage of tungsten increases to about 45–50 at.% at a depth of ~0.5 μm, where it is equal to the carbon levels. As the carbon layer approaches the surface, it approaches 90 at.%, the tungsten content decreasing to 10 at.% and remaining constant for the last 0.2 μm below the surface.

As can be seen in Figure 3, in the sample pretreated at 350°C, the depth of nitrogen reaches 7.5 μm and an atomic concentration of 17.5% of nitrogen. This signal goes even deeper in the sample pretreated at 400°C, reaching a depth of approximately 10 μm with an initial higher concentration of about 20% of nitrogen, and in the sample pretreated at 450°C presents a depth up to 16.5 μm with an initial concentration of about 22.5%.

The surface roughness (Sa) of duplex coatings processed at different temperatures has been studied. From Sa 43.8 ± 7.4 nm for the simple DLC sample, a lower roughness of 28.3 ± 4.3 nm with pretreatment at 350°C is observed, rising to Sa 75.1 ± 5.5 nm at 400°C and experiencing a maximum roughness Sa of 94.9 ± 27.4 nm with 450°C. This increase in roughness is directly related to the increase in ion bombardment of plasma of higher current density with increasing treatment temperature. The roughness could be reduced by applying a higher positive voltage or achieving a lower roughness in the initial polishing of the sample [19].

2.2. Nanoindentation Test. Hardness (H), Young's modulus (E), $H\ E^{-1}$ (resistance to elastic deformation), and H^3E^{-2} (resistance to plastic deformation, where E is a function of Poisson's ratio [25]) ratios have been calculated the AISI-316L reference sample and the WC : C coatings (Table 1).

The hardness of the substrate is 3.0 GPa, increasing in the simple DLC coating up to 17.4 GPa. In the samples subjected to pretreatment,hardness is maintained at similar values, decreasing the average but increasing the margin of error due to the increase in roughness. They have been calculated at 16.2, 16.1, and 14.7 GPa for 350°C, 400°C, and 450°C, respectively, with standard deviation margins of 1.7–1.9 GPa. In the load-depth curves shown in Figure 4, a high elasticity component can be observed for the WC : C coatings, both as stand-alone coating or with duplex treatments (144.2–161.5) as studied by J.A. Garcia et al. [24].

2.3. Adhesion Test. To determine the adhesion of the coating, scratch tests with loads increasing from 0 to 100 N were carried out on a length of 10 mm. Different failure modes were observed along with the scratches and loads to which they were subjected were recorded. All tests show high adhesive behavior.

Figure 5 represents the acoustic emission (AE) and the coefficient of friction (COF) along with the scratch tests of the 400°C pretreated sample, which assumes the relationship between the normal and tangential forces when the penetrator plows the surface while the normal load is constantly increased. Due to surface inhomogeneities, the first cohesive failure (LC1) has been extremely difficult to detect.

The first adhesive failure LC2 of the simple DLC WC : C was 27.5 ± 1.5 N, for the 350°C ASPN + WC : C was measured in 9.2 ± 0.4 N, for 400°C this failure went up to 11.5 ± 0.7 N, and for the 450°C it finally rose to 27.5 ± 0.7 N. In the DLC WC : C coating, the total delamination LC3 (micrograph of the total delamination failures is shown in Figures 6(a)–6(d)) showed values of 48.5 ± 3.5 N. In samples pretreated using active screen plasma nitriding, the said delamination depends on the temperature of the treatment. In the case of 350°C, the values reached up to 34.5 ± 0.7 N. For 400°C, values of 82.0 ± 2.6 N were achieved, and for the pretreatment of 450°C, they reached up to 75.3 ± 7.8 N (Figure 7), albeit with a larger standard deviation, where two scratches have been measured and this could be due to the

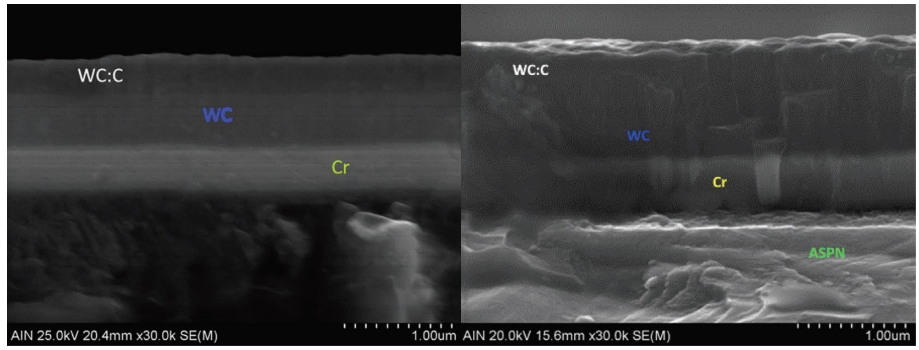

Figure 1: Cross section SEM picture with the coating's structure of DLC WC : C (a) and ASPN 400°C + DLC WC : C (b). From the bottom to top, the image shows the stainless-steel substrate, the bonding layer of Cr, the WC interlayer, and the W-doped layer.

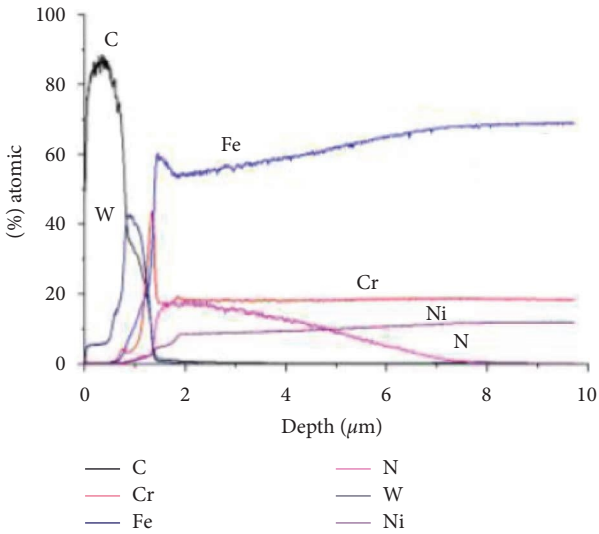

Figure 2: Glow discharge optical emission spectrometry (GDOES) concentration profile of ASPN 350°C + DLC WC : C coating.

differences between the roughness of each surface on this last type of coating.

For adherence LC3 over a stainless steel substrate, the adhesion overall reaches higher values than the PVD Cr-DLC processes reported by F.D. Duminica with 35 N or in studies by Zhou et al. with Ti DLC coatings with 35.8 N [26–29]. In the study with low temperature (lower than 400°C) carburization DLC coatings manufactured by Zhou et al. for a-C : H, the LC3 was 49 N with a thickness of 3.8 μm [27]. It can also be seen that this nitriding technique is more efficient for improving adhesion than the plasma ion immersion implantation technique as shown by Iñigo et al. with a maximum of 38.7 N LC3 [19].

2.4. Friction and Wear Test. As seen in Figure 8, the coefficient of friction (COF) of all the samples is quite low and much lower than for the control, untreated stainless-steel substrate. Simple DLC sample COF was measured at 0.1 as seen in other studies [19, 30]. The coefficient of friction for ASPN 350°C + DLC was 0.07, for ASPN 400°C + DLC was 0.08, and for 450°C was 0.12. For 350°C and 400°C, COF results are lower and smoother than for simple WC : C DLC samples, which means that this type of coating is improving their properties by avoiding as much as possible opposition to sliding on it. The Daimler–Benz test carried out in concordance with VDI 3198 confirms the types of faults analyzed in the scratch tests. Figure 9(a) shows us an HF1 with cohesive failures and a homogeneous crater border, Figure 9(b) shows us an HF6 with an adhesive catastrophic failure, Figure 9(c) shows us an HF3 with an increase of cohesive failures and an inhomogeneous crater border, and Figure 9(d) shows us an HF1 with a homogeneous crater border with some cohesive failures [31].

For the volume loss in wear tracks similar data (Table 2) on all the duplex samples can be seen on Figure 10. Samples have a 1.18×10^{-12}, 1.82×10^{-12}, and 2.19×10^{-12} m^3 volume loss for 350°C, 400°C, and 450°C. These results imply similar volume losses to those in a simple DLC sample with a 4.35×10^{-13} m^3 loss. The wear coefficient of the coatings was also measured with a result of $4.5 \pm 2.4 \times 10^{-7}$ mm^3 N^{-1} m^{-1} for the 350°C, $7.9 \pm 3.7 \times 10^{-7}$ mm^3 N^{-1} m^{-1} for the 400°C, and $14.4 \pm 10.0 \times 10^{-7}$ mm^3 N^{-1} m^{-1} for the 450°C, like the 4.0 ± 1.0 10^{-7} mm^3 N^{-1} m^{-1} of the simple DLC coating. The greater the roughness in samples such as those of 400°C and 450°C, the greater the error in the measurements found.

2.5. Stress Test. The XRD spectra, depicted in Figure 11, show the presence of main austenite (γ) in the untreated AISI 316L sample, together with some martensite, which is explained by the mirror polishing process [19]. In the case of the nitrided samples, expanded austenite (γN) is also present, and some nitride precipitates can be observed at the higher treatment temperature of 450°C. In addition, a growing deviation toward smaller angles can be observed on the (200) expanded austenite peaks as the nitriding temperature increases, which indicates an increase in residual stresses. A deviation to lower angles is also observed in the (111) peak of expanded austenite in the 400°C nitrided sample as compared to the one nitrided at 350°C, but not from 400°C to 450°C. This might be related to the influence of a larger faulting gradient in the 450°C nitrided sample. DLC HiPIMS with positive pulses coating with 350 V and 150 Hz has higher internal stress than other voltages as exposed by Verein–Deutscher–Ingenieure improving the hardness of the film but decreasing the deposition rate and

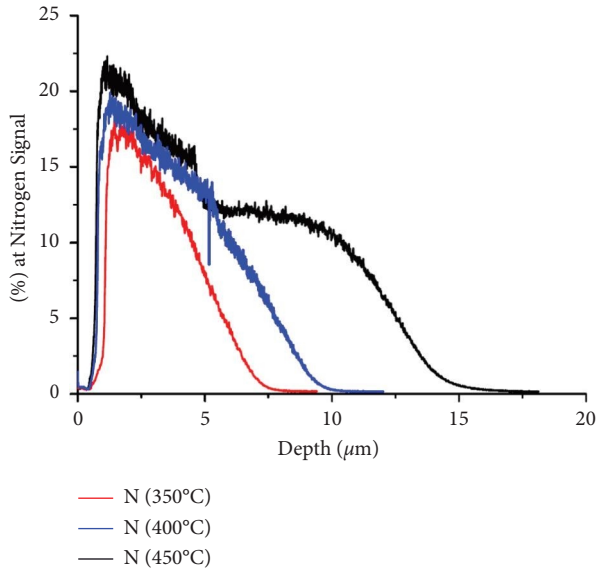

Figure 3: GDOES concentration depth profiles of nitrogen over the ASPN + DLC concentration profile.

Table 1: Reference, DLC WC : C, and ASPN + DLC nanoindentation results for hardness (H), Young's modulus (E), and their relationship $H\,E^{-1}$ and H^3E^{-2}.

Types of samples	H (GPa)	E (GPa)	$H\,E^{-1}$	$H^3\,E^{-2}$ (MPa)
Reference	3.0 ± 0.1	110.0 ± 5.0	0.027	2.2
DLC WC : C	17.4 ± 0.4	161.5 ± 2.5	0.108	201.9
ASPN 350°C + DLC	16.2 ± 1.7	147.8 ± 10.7	0.110	194.6
ASPN 400°C + DLC	16.1 ± 1.7	146.6 ± 10.3	0.107	194.2
ASPN 450°C + DLC	14.7 ± 1.9	144.2 ± 13.8	0.102	152.7

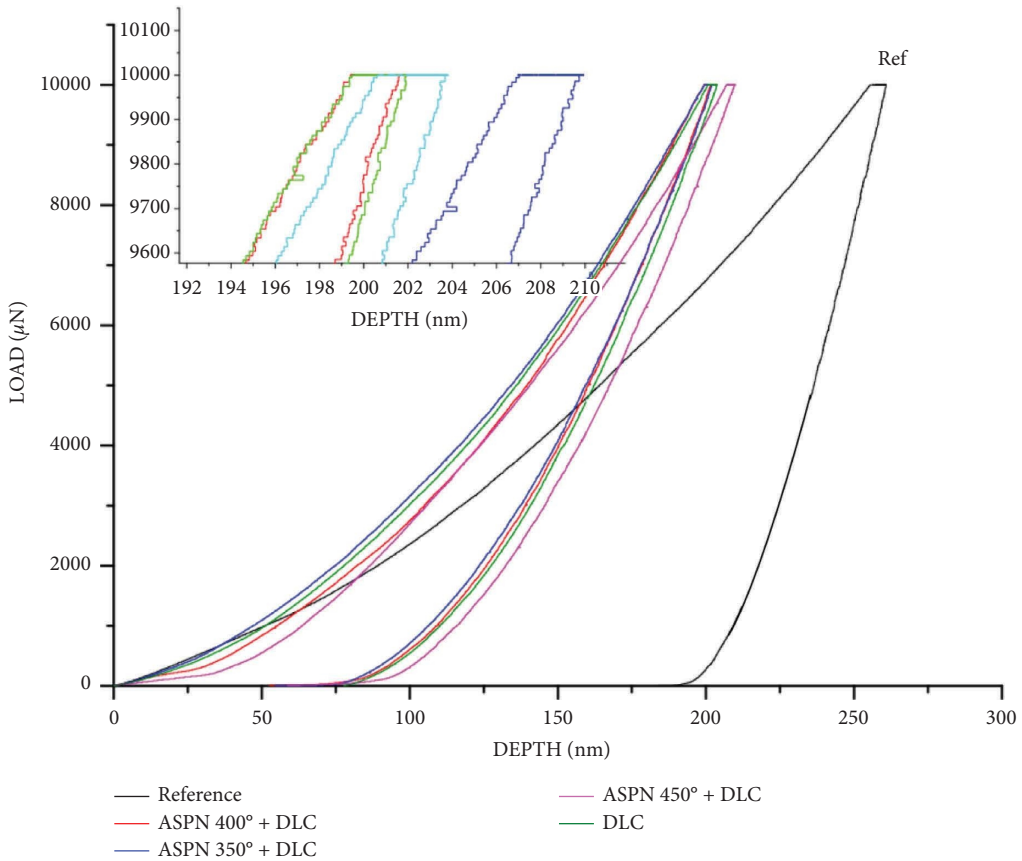

Figure 4: Nanoindentation curves of the WC : C coating (light blue plot), ASPN 350°C + DLC (light green plot), ASPN 400°C + DLC (red plot), ASPN 450°C + DLC (dark blue plot), and reference AISI316-L (dark green plot) (10 mN).

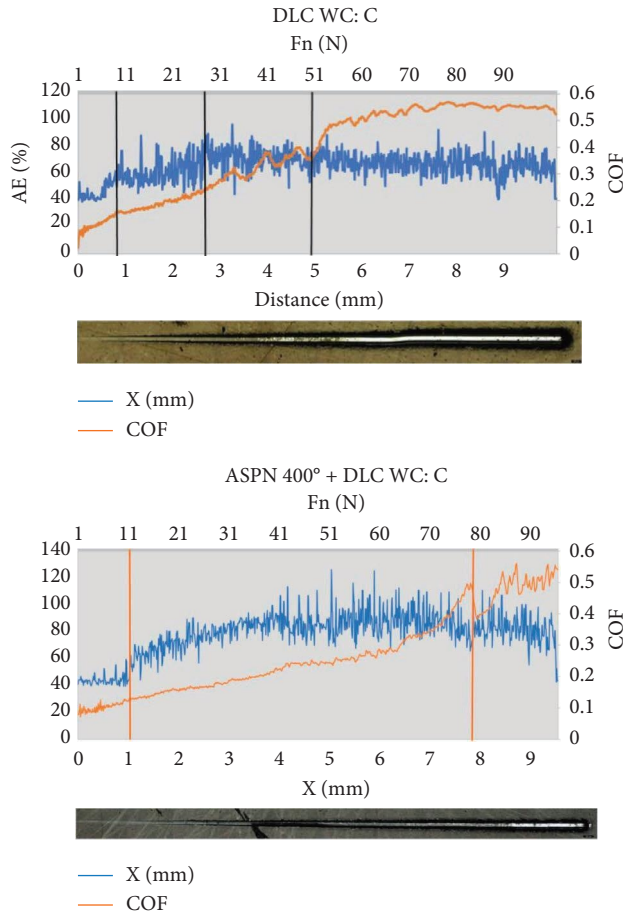

Figure 5: Acoustic emission evolution of DLC coating and ASPN with pretreatment at 400°C + DLC WC : C (COF: blue plot and AE: orange plot) vs. the indenter displacement. (a) DLC WC : C. (b) ASPN 400°C + DLC WC : C.

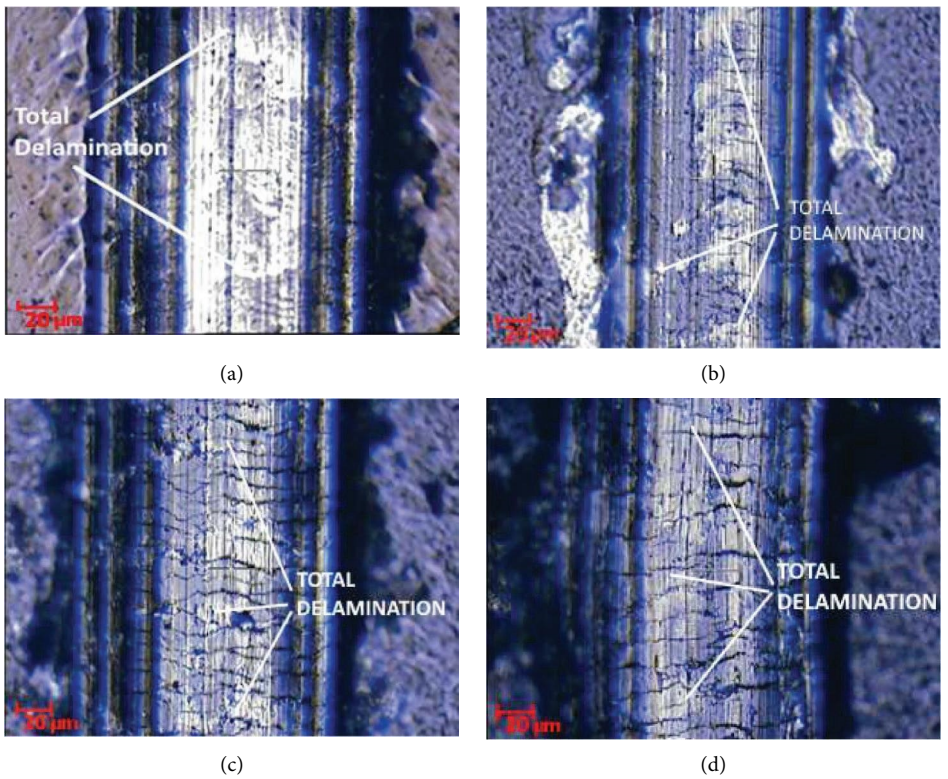

(a) (b)

(c) (d)

Figure 6: Scratch test micrography of DLC WC : C (a), ASPN 350°C + DLC (b), ASPN 400°C + DLC (c), and ASPN 450°C + DLC (d).

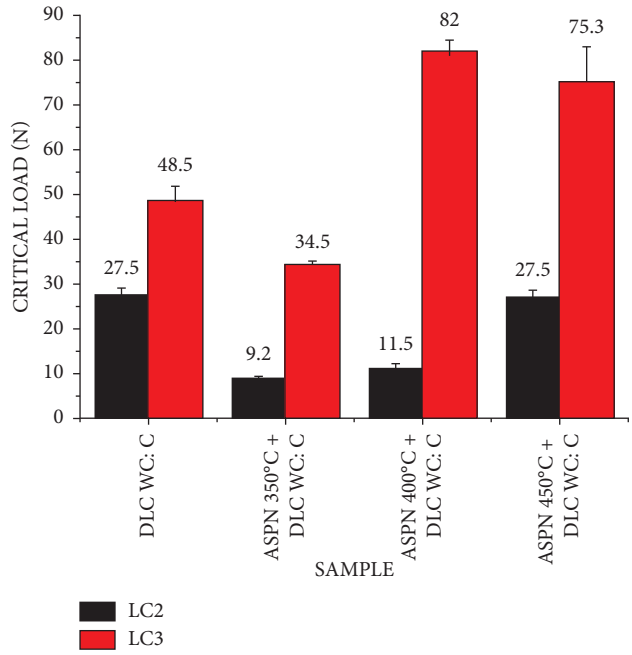

Figure 7: Experimental data derived from the scratch test with the corresponding values of critical load (LC2 and LC3) for DLC WC : C coating sample.

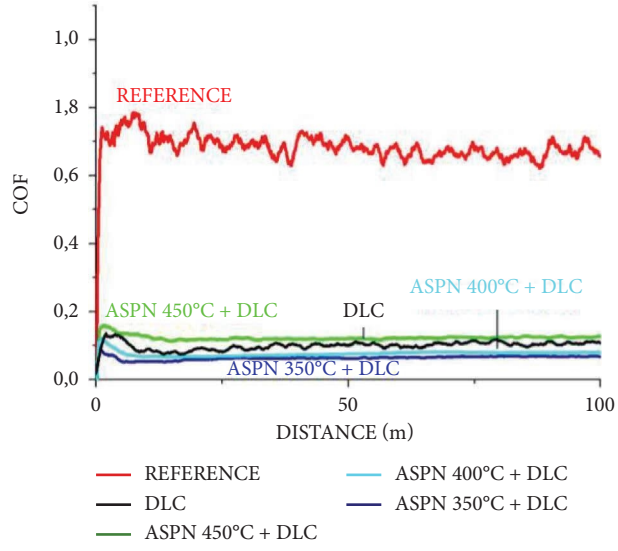

Figure 8: Friction coefficients of DLC sample (black plot), ASPN 450°C + WC : C coating (green plot), ASPN 400°C + WC : C coating (light blue plot), ASPN 350°C + WC : C coating (dark blue plot), and reference AISI316-L (green plot).

improving the residual compressive stresses which influence impacts in the wear resistance behavior [32].

3. Discussion

The adherence of DLC coatings made using the HiPIMS technique on 316 L stainless steel has been tested reaching LC2 values of 27.5 N and LC3 values of 48.5 N. If nitriding techniques are previously carried out using active screen plasma nitriding, LC3 values increase up to 80N, although the final value depends on the treatment temperature. The LC2 value remained for the treatments carried out at 450°C, where the values at the same range as the 28 N achieved with the HiPIMS technique in the simple DLC coating.

Nitriding increased the roughness, despite this there were results where the adherence of the coating was increased, which indicates the efficacy of the tested treatment. Adhesion, as measured per LC3, increased at ASPN 400°C + DLC and at ASPN 450°C + DLC, assisted by larger roughnesses and more stress gradients. LC2 stayed at low values in ASPN400°C + DLC as opposed to the ASPN 450°C + DLC sample, which showed roughly the same LC2

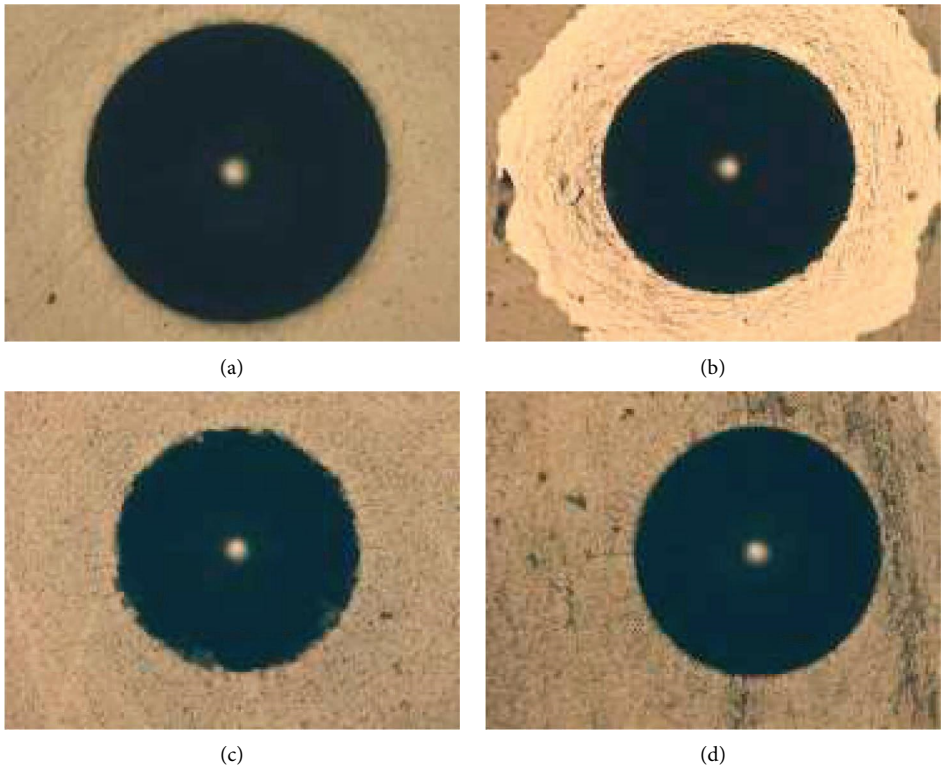

Figure 9: Daimler–Benz rockwell-C adhesion test chart of DLC (a), ASPN 350°C + DLC (b), ASPN 400°C + DLC (c), and ASPN 450°C + DLC (d).

Table 2: Summary of the experimental data of volume loss and wear coefficient measured by confocal microscopy.

Types of samples	Width of wear track (μm)	Wear coefficient ($mm^3\ Nm^{-1}$)
DLC WC : C	110 ± 5	$4.0 \pm 1.0 \times 10^{-7}$
ASPN 350°C + DLC WC : C	80 ± 2.5	$4.5 \pm 2.4 \times 10^{-7}$
ASPN 400°C + DLC WC : C	80 ± 2.5	$7.9 \pm 3.7 \times 10^{-7}$
ASPN 450°C + DLC WC : C	70 ± 2.5	$14.0 \pm 10.0 \times 10^{-7}$

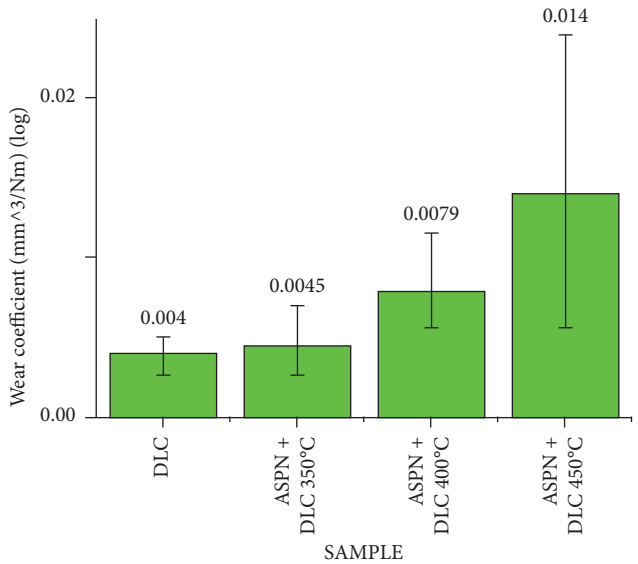

Figure 10: Wear coefficient ($mm^{-3}\ Nm^{-1}$) of DLC coating reference and ASPN + DLC samples.

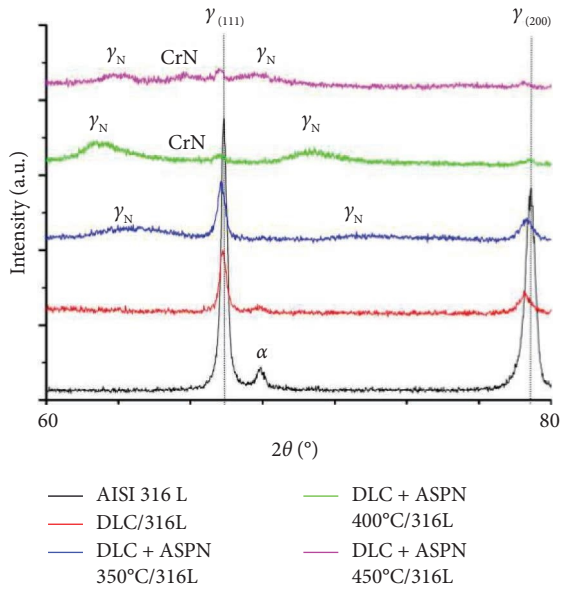

Figure 11: Chromium Ka source X-ray diffraction pattern of AISI316L, WC : C DLC coating, and ASPN + DLC coatings at 350°C, 400°C, and 450°C.

Table 3: AISI316L chemical composition.

AISI-316L	C	Cr	Ni	Mo	Si	Mn	Fe
%	0.022	16.50	10.08	2.02	0.41	1.56	Bal.

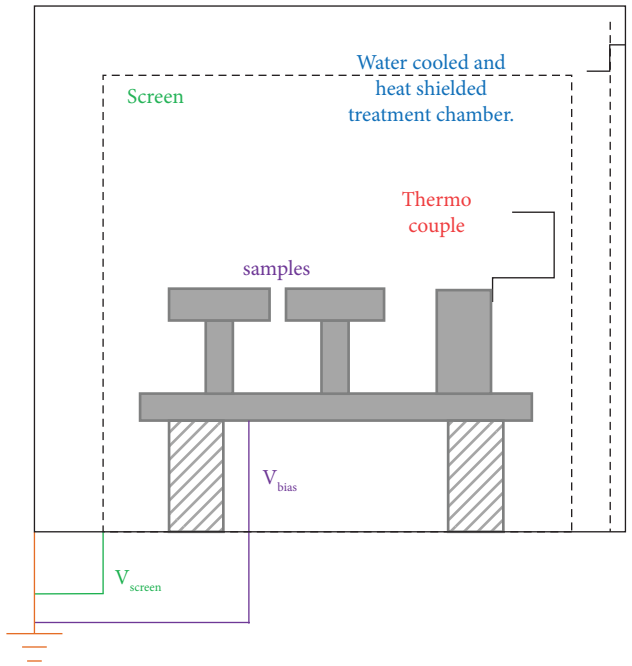

Figure 12: Scheme of the active screen plasma nitriding reactor.

value as the DLC sample. The fact that there is a larger presence of stacking faults in ASPN 450°C + DLC might have assisted in stress relive in the DLC coating and thus to a smoother gradient of stresses across the whole section. The presence of nitride precipitates might have also played a role, although further studies are necessary to determine the causes behind the different adhesion properties observed [33].

From the tribological point of view, the application of the coating shows an improvement in the wear resistance compared to the original substrate and the wear rate remains quite similar when applying the nitriding pretreatment. It should be considered retrospectively that the tribo-test conditions were quite mild, i.e., the wear remained within the DLC coat thickness and no delamination effect or coating collapse was observed in any sample, that could have been the case under more severe conditions.

The coefficient of friction in some duplex treatments (at 350°C and 400°C) is lower than those provided by the samples only treated with DLC [23]. Moreover, the evolution of friction along the test is also far smoother. As indicated in the studies of Christiansen et al. [33], the compressive stress of the DLC layer decreases when suffering cohesive failures in the coating, allowing an improvement in the coefficient of friction through the appearance of carbon remains in the wear marks. The adhesion between the deposition caused by the ASPN increases the maximum critical load Lc3, assuming an improvement in the adhesion between the substrate and the nitrided layer as well as between the nitrided layer and the deposited DLC.

This study has shown that the appropriate parameters of the active screen plasma nitriding treatment could achieve the optimum point between adhesion of the DLC coating, the lowest coefficient of friction, and the highest resistance to wear. In the case of the parameters analyzed in this study,

results indicate that the 400°C nitriding pretreatment temperature offers the best compromise between the adherence (Lc3 of 82 N), a COF smooth below 0.1, and a wear rate coefficient of the order of the original DLC, which maintains and improves the properties of the tested simple DLC coating.

4. Conclusion

In this work, an improvement in adhesion without a significant decrease in wear resistance has been achieved with duplex coatings of similar coefficient of friction formed through an active screen plasma nitriding layer and a DLC WC : C coating deposited using the technique positive pulse HiPIMS in AISI316L stainless steel. The temperature of the nitriding process affected the final roughness of the coatings influencing the compressive stress and adherence but it has not influenced the COF. The wear coefficient has maintained its properties in the different studied parameters like DLC coating. The critical load failure has reached up to 82 N and 75.3 N with higher temperature parameters almost duplicating the original DLC critical load.

More studies are needed to achieve the succeeded temperature parameter to improve all the duplex treatment tribological properties.

5. Experimental Section/Methods

5.1. Reference Substrates. The samples are made of AISI 316L surgical stainless steel, the chemical composition of which is detailed in Table 3. Made in a flat geometry with a diameter of 30 mm, a surface mirror polish was performed with a final roughness (Ra) of less than 0.2 microns using sequential sanding with sandpaper grits from 320 to 1200 and 6, 3, and 1 μm grain suspended diamond cloth. Lastly, alumina was used for the final mirror polish. After this, ultrasonic cleaning was carried out in baths with alkaline detergents, cleaned with deionized water, and rinsed with isopropanol to subsequently dry them using dry air.

5.2. Active Screen Plasma Nitriding. The samples were subjected to active screen plasma nitriding processes, which were carried out in self-built nitriding equipment at the Surface Engineering Laboratory of Tecnalia, as seen in Figure 12 [1, 34]. In the active screen plasma treatments, the outer screen is subjected to a voltage, while the samples are immersed in plasma and biased to a lower potential.

The samples were initially plasma cleaned with 50 : 50 Ar : H2 gas mix for 140 minutes, at a pressure of approximately 200 Pa, to remove residual surface contaminants and the naturally occurring surface oxides, applying a bias voltage of −305 V (and −215 V in the screen). Subsequently, nitriding processes followed, with a 25 : 75 $N_2 : H_2$ gas mix, at 170 ± 10 Pa. Applying bias voltages of −600 V, −725 V, and −880 V, in combination with screen currents of 4.5 A, 4.7 A, and 5.0 A (−505 V), resulted in nitriding process temperatures of 350°C, 400°C, and 450°C during 7.5, 4, and 1.5 hours, respectively. The process temperatures were monitored by a thermocouple in an adjoining bulk dummy cylinder, positioned like the samples (i.e., similar distance to the screen). After the plasma nitriding processes were completed, samples were cooled down in a vacuum.

5.3. DLC Deposition Technique. The DLC coatings have been deposited in a custom-made batch-type coating system designed and manufactured by Nano4Energy S.L. Chamber diagram has been shown by Iñigo et al. with a configuration that integrates a 0.6 m^3 vacuum chamber with three rectangular cathodes of Cr, WC : C, and C [19].

The vacuum is carried out by means of turbomolecular pumps in addition to two-stage rotary vane pumps, achieving a pressure of 10^{-4} Pa. The process is the same as that described in the study by Iñigo et al. [19].

(1) Argon etching: Ar + discharge is performed on the substrates for 15 minutes, with a direct current (DC) pulsed polarization voltage of −500 V and a frequency of 150 kHz.

(2) Deposition of Cr-HiPIMS bonding layer: The Cr target is powered with pulses of 150 μs, a repetition frequency of 300 Hz, and an average power density of 5 W/cm^2. The deposition rate was measured as 0.5 μm/h for a three-fold rotation with a substrate voltage bias of −50 V.

(3) Deposition of an intermediate layer of WC : The WC was deposited by means of direct current (DC) pulsed magnetron sputtering with a power density of 7.5 W/cm^2, a frequency of 150 kHz, and a pulse width of 2.7 μs. The substrate bias was kept at −50 V. The deposition speed obtained for a 3-fold rotation was 0.38 μm/h.

(4) W-doped DLC coating deposition: Carbon layers were codeposited with WC layers. The power density of the pulses was up to 10 W/cm^2. The carbon target was powered by DC-pulsed technology at a repetition frequency of 150 kHz and a pulse width of 2.9 μs. The HiPIMS mode was applied to a WC : C target with a pulse time of 150 μs, a repetition frequency of 300 Hz, a positive pulse of 350 V, and a power density of 0.5 W/cm^2. A substrate voltage bias of −50 V was applied. The deposition rate obtained for a three-fold rotation was 0.25 μm/h.

5.4. Thickness, Structural Properties, and Profile Composition. Glow discharge optical emission spectroscopy (GDOES) has been used to determine the chemical composition profile with JOBIN YVON 100000RF equipment (HORIBA Instruments, Tokyo, Japan) [30]. The phase formation with the ASPN was evaluated by means of the X-ray diffraction with chromium K_a source XRD D8 DISCOVER (Bruker, Billerica, Massachusetts, USA) with a variable output slit at 0.5 and 1 mm diameter collimator. After diffraction, it passes through another open variable slit at 5 mm and a vanadium filter to remove K_{a2} and ends up in the fully open Lynxeye detector in 1D configuration. For the images of the cross section, a HITACHI S4800 field emission scanning electron

microscope (FE-SEM) (HITACHI High-Technologies Corporation, Tokyo, Japan) has been used. The thicknesses of the coatings were corroborated with the CSM Calotest equipment (CSM Instruments, Peseux, Switzerland) using stainless steel balls of 30 mm in diameter and superfine diamond water suspension as the abrasive medium.

5.5. Roughness, Mechanical, and Tribological Tests. The nanoindentation tests have been carried out by Hysitron Triboindenter TI 950 (Hysitron, Eden Prairie, Minnesota, USA) fitted with a Berkovich tip with a final radius of 150 nm. Hardness and Young's modulus were studied following the method of Oliver and Pharr using indentations of 10 mN of maximum load, $H\,E^{-1,}$ and H^2E^{-3} ratios have been related according to the studies carried out by Santiago et al. [33, 34]. To evaluate the adhesion between the substrate and coating, scratch tests were carried out with a REVETEST CSM equipped with a Rockwell EURO 150518C&N penetrator of 200 μm of tip radius, using loading rates of 100 N/min, with a speed of 100 mm/min, and a final load of 100 N. Three scratches were performed per sample.

The signals recorded when making the scratches were depth, acoustic emission, and friction coefficient. In this test, three different critical loads are considered, but not always is possible to detect all three. The first critical load (LC1) is registered at the point where the first crack is seen on the surface of the coating, but no delamination has been produced. The second critical load (LC2) marks the load at which the first adhesive failure is detected, normally some chipping at the edges of the track. Finally, the third critical load (LC3) is identified when the delamination of the coating is catastrophic, and the coating no longer supports the load of the indenter.

Adhesion was measured additionally using the Daimler–Benz Rockwell-C adhesion test following the VDI-3198 standard [30] with a durometer Instron Testor 930-250 (Instron Wolpert GmbH, England). It uses a standard Rockwell hardness tester, with a Rockwell type C diamond cone indenter with an applied load of 150 kg. The indentations were observed under an optical microscope and classified according to the adhesion between HF1 and HF6 according to the level of cracking and delamination of the coating around the indentation.

The surface roughness (Sa) was measured in a smart confocal microscope (Sensofar, Spain) under the ISO25178 standard with a 50X objective. The lengths used were 1600–1750 μm and the following filters were used to obtain the surface roughness values (according to the ISO 25178 standard):

(i) Standard cutoff of the high pass filter: $\lambda_s = 2.50\,\mu$m

(ii) Standard cutoff of the low pass filter: $\lambda_c = 0.08$ mm

For the study, three 3D noncontact area measurements were performed in three areas of the sample.

For the tribomechanical tests, a microtest equipment in pin-on-disk configuration with a 6 mm alumina ball loaded at 2–5 N, 200 rpm, and 6,000–8,000 cycles were used to find the coefficient of friction (COF) under similar humidity conditions. The study of the wear marks, as well as the volume loss, were measured using a smart confocal microscope (Sensofar, Spain) under the ASTM99 standard.

Tribological and XRD data used to support the findings of this study have been deposited in the FAIRsharing repository https://fairsharing.org/4429 and https://fairsharing.org/users/7831.

FAIRsharing.org: tribology duplex; tribology duplex ASPN + DLC WC : C, FAIRsharing ID https://fairsharing.org/4429, last edited on Sunday, September 25th 2022, 13:44, the last editor was Igomez, and last accessed on Sunday, September 25th 2022, 14:06.

Data Availability

Data are available from the corresponding author on request.

Conflicts of Interest

The authors declare that they have no conflicts of interest.

Authors' Contributions

Iñigo Gómez Alonso and Jose Antonio Garcia Lorente contributed equally to this work. Conceptualization, methodology, formal analysis, research, resources, writing-original draft preparation, writing-review and editing, project administration, and funding acquisition were done by Iñigo Gómez. Methodology, formal analysis, investigation, writing-original draft preparation, writing-review and editing, supervision, and funding acquisition were done by Jose Antonio Garcia. Research, writing-review, and editing were done by Jose Antonio Santiago. Investigation and writing-review were done by Iván Fernandez. Investigation, writing-review, and editing were done by Jose Fernandez. Research, writing-review, and editing were done by Iñigo Braceras. All authors have read and agreed to the published version of the manuscript.

Acknowledgments

This research was supported by the Government of Navarra grants for hiring doctoral students (Iñigo Gómez) by companies and research and knowledge dissemination organizations: industrial doctorates 2019–2021, grant no. 0011-1408-2018-000000 and CDTI Ministerio de Ciencia e Innovación of Spain through the project CERVERA (CER2019-1003).

References

[1] B. AlMangour, D. Grzesiak, and J. M. Yang, "Selective laser melting of TiB2/316l stainless steel composites," *The Roles of Powder Preparation and Hot Isostatic Pressing Post-Treatment*, vol. 309, 2017.

[2] R. J. Miron and D. D. Bosshardt, "OsteoMacs: key players around bone biomaterials," *Biomaterials*, vol. 82, pp. 1–19, 2016.

[3] D. Goutallier, "The history of knee prosthesis," *La Revue du praticien*, vol. 41, no. 16, pp. 1431–1435, 1991.

[4] N. Bruns and C. Krettek, "3D-printing in trauma surgery: planning, printing and processing," *Unfallchirurg, Der*, vol. 122, no. 4, pp. 270–277, 2019.

[5] R. Shah, B. Gashi, S. Hoque, M. Marian, and A. Rosenkranz, "Enhancing mechanical and biomedical properties of protheses - surface and material design," *Surfaces and Interfaces*, vol. 27, Article ID 101498, 2021.

[6] B. Dong, X. Guo, K. Zhang et al., "Combined effect of laser texturing and carburizing on the bonding strength of DLC coatings deposited on medical titanium alloy," *Surface and Coatings Technology*, vol. 429, no. 1, Article ID 127951, 2022.

[7] M. Kaneko, M. Hiratsuka, A. Alanazi, H. Nakamori, K. Namiki, and K. Hirakuri, "Surface reformation of medical devices with DLC coating," *Materials*, vol. 14, no. 2, pp. 376–410, 2021.

[8] K. Sakurai, M. Hiratsuka, H. Nakamori, K. Namiki, and K. Hirakuri, "Evaluation of sliding properties and durability of DLC coating for medical devices," *Diamond and Related Materials*, vol. 96, pp. 97–103, 2019.

[9] K. Bewilogua and D. Hofmann, "History of diamond-like carbon films - from first experiments to worldwide applications," *Surface and Coatings Technology*, vol. 242, pp. 214–225, 2014.

[10] A. Boulila, K. Jendoubi, A. Zghal, M. Khadhraoui, and P. Chabrand, "Comportement mécanique des prothèses totales de hanche au pic de chargement," *Mécanique & Industries*, vol. 11, no. 1, pp. 25–36, 2010.

[11] S. Aisenberg and R. Chabot, "Ion-beam deposition of thin films of diamondlike carbon," *Journal of Applied Physics*, vol. 42, no. 7, pp. 2953–2958, 1971.

[12] J. A. García, C. Díaz, S. Mändl, J. Lutz, R. Martínez, and R. J. Rodríguez, "Tribological improvements of plasma immersion implanted CoCr alloys," *Surface and Coatings Technology*, vol. 204, no. 18-19, pp. 2928–2932, 2010.

[13] J. A. Santiago, I. Fernández-Martínez, J. C. Sánchez-López et al., "Tribomechanical properties of hard Cr-doped DLC coatings deposited by low-frequency HiPIMS," *Surface and Coatings Technology*, vol. 382, Article ID 124899, 2020.

[14] J. A. Santiago, I. Fernández-Martínez, A. Wennberg et al., "Adhesion enhancement of DLC hard coatings by HiPIMS metal ion etching pretreatment," *Surface and Coatings Technology*, vol. 349, pp. 787–796, 2018.

[15] Y. Li, Y. He, W. Wang et al., "Plasma nitriding of AISI 304 stainless steel in cathodic and floating electric potential: influence on morphology , chemical characteristics and tribological behavior," *Journal of Materials Engineering and Performance*, vol. 27, no. 3, pp. 948–960, 2018.

[16] C. X. Li and T. Bell, "Corrosion properties of active screen plasma nitrided 316 austenitic stainless steel," *Corrosion Science*, vol. 46, no. 6, pp. 1527–1547, 2004.

[17] C. Zhao, C. X. Li, H. Dong, and T. Bell, "Study on the active screen plasma nitriding and its nitriding mechanism," vol. 201, pp. 2320–2325, 2006.

[18] S. Patel, B. Ganguli, and S. K. Chaudhury, "Active screen plasma nitriding characteristics of 347H austenitic stainless steel," *Transactions of the Indian Institute of Metals*, vol. 75, no. 3, pp. 663–671, 2022.

[19] G. Iñigo, A. Santiago, J. F. Palacio, C. Diaz, S. Mändl, and J. A. Garcia, "Improved adhesion of the DLC coating using HiPIMS with positive pulses and plasma immersion pretreatment," *Coatings*, vol. 11, no. 9, p. 1070, 2021.

[20] X. Kuang, L. Li, L. Wang, G. Li, K. Huang, and Y. Xu, "The effect of N+ ion-implantation on the corrosion resistance of HiPIMS-TiN coatings sealed by ALD-layers," *Surface and Coatings Technology*, vol. 374, pp. 72–82, 2019.

[21] W. Tillmann, N. F. Lopes Dias, and D. Stangier, "Influence of plasma nitriding pretreatments on the tribo-mechanical properties of DLC coatings sputtered on AISI H11," *Surface and Coatings Technology*, vol. 357, pp. 1027–1036, 2019.

[22] I. Braceras, I. Ibáñez, S. Dominguez-Meister et al., "Plasma nitriding of the inner surface of stainless steel tubes," *Surface and Coatings Technology*, vol. 355, pp. 116–122, 2018.

[23] F. Avino, D. Fonnesu, T. Koettig et al., "Improved film density for coatings at grazing angle of incidence in high power impulse magnetron sputtering with positive pulse," *Thin Solid Films*, vol. 706, Article ID 138058, 2020.

[24] J. A. García, P. J. Rivero, E. Barba et al., "A comparative study in the tribological behavior of DLC coatings deposited by HiPIMS technology with positive pulses," *Metals*, vol. 10, no. 2, p. 174, 2020.

[25] A. Leyland and A. Matthews, "On the significance of the H/E ratio in wear control: a nanocomposite coating approach to optimised tribological behaviour," *Wear*, vol. 246, no. 1-2, pp. 1–11, 2000.

[26] Y. Zhou, L. Li, W. Shao et al., "Mechanical and tribological behaviors of Ti-DLC films deposited on 304 stainless steel: exploration with Ti doping from micro to macro," *Diamond and Related Materials*, vol. 107, Article ID 107870, 2020.

[27] I. Boromei, L. Ceschini, A. Marconi, and C. Martini, "A duplex treatment to improve the sliding behavior of AISI 316L: low-temperature carburizing with a DLC (a-C: H) topcoat," *Wear*, vol. 302, no. 1-2, pp. 899–908, 2013.

[28] F. D. Duminica, R. Belchi, L. Libralesso, and D Mercier, "Investigation of Cr(N)/DLC multilayer coatings elaborated by PVD for high wear resistance and low friction applications," *Surface and Coatings Technology*, vol. 337, 2018.

[29] T. Fu, Z. F. Zhou, Y. M. Zhou et al., "Mechanical properties of DLC coating sputter deposited on surface nanocrystallized 304 stainless steel," *Surface and Coatings Technology*, vol. 207, pp. 555–564, 2012.

[30] J. A. García, R. J. Rodríguez, R. Martínez, C. Fernández, A. Fernández, and R. Payling, "Depth profiling of industrial surface treatments by rf and dc glow discharge spectrometry," *Applied Surface Science*, vol. 235, no. 1-2, pp. 97–102, 2004.

[31] Verein-Deutscher-Ingenieure, "Verein deutscher ingenieure daimler benz adhesion test, VDI 3198," *Dusseldorf: VDI-Verlag*, Springer, New York, NY, USA, 1992.

[32] T. L. Christiansen, T. S. Hummelshøj, and M. A. J. Somers, "Expanded austenite, crystallography and residual stress," *Surface Engineering*, vol. 26, no. 4, pp. 242–247, 2010.

[33] J. A. Santiago, I. Fernández-Martínez, T. Kozák et al., "The influence of positive pulses on HiPIMS deposition of hard DLC coatings," *Surface and Coatings Technology*, vol. 358, pp. 43–49, 2019.

[34] I. Braceras, I. Ibáñez, S. Domínguez-Meister et al., "Corrosion preserving high density plasma treatment of precipitation hardening stainless steel," *Surface and Coatings Technology*, vol. 355, pp. 174–180, 2018.